

Highly Oriented 1-D ZnO Nanorod Arrays on Zinc Foil: Direct Growth from Substrate, Optical Properties and Photocatalytic Activities

Yuxin Wang,[†] Xinyong Li,^{*,†,‡} Guang Lu,[†] Xie Quan,[†] and Guohua Chen[‡]

Key Laboratory of Industrial Ecology and Environmental Engineering and State Key Laboratory of Fine Chemical, School of Environmental and Biological Sciences and Technology, Dalian University of Technology, Dalian 116024, China, and Department of Chemical Engineering, Hong Kong University of Science & Technology, Clear Water Bay, Kowloon, Hong Kong, P. R. China

Received: November 29, 2007; In Final Form: January 20, 2008

Highly oriented and large-scale ZnO nanorod arrays have been successfully synthesized on zinc foil by a simple, low-temperature, solution-phase approach. In this approach, zinc foil was used not only as a substrate but also as a zinc-ion source for the direct growth of ZnO nanorod arrays. X-ray diffraction (XRD) analysis, high-resolution TEM (HRTEM) images, and selected-area electron diffraction (SAED) patterns indicated that the structure of the ZnO nanorod arrays on the zinc foil substrate was single-crystalline and grown in the [0001] direction with a wurtzite structure. The optical properties of the ZnO nanorod arrays were characterized by UV–vis diffuse reflectance, Raman, and photoluminescence spectroscopies. The photocatalytic activity of the ZnO nanorod arrays was tested by degradation of 4-chlorophenol (4-CP) under UV light irradiation compared to that of a ZnO nanorod film grown on a Ti substrate, indicating that the as-synthesized ZnO nanorod arrays exhibit excellent photocatalytic activity.

1. Introduction

ZnO has been recognized as one of the most important multifunctional semiconductor materials for its wide band gap ($E_g = 3.37$ eV) and large excitonic binding energy (60 meV) at room temperature. Particularly, one-dimensional (1-D) ZnO nanostructures such as wires, rods, belts, tubes, and whiskers have been extensively studied because of their functional applications in electronic and optoelectronic devices,¹ gas sensors,² field-emission devices,³ solar cells,⁴ and photocatalysts.⁵

ZnO, as a well-known photocatalyst, has been the focus of much attention in the degradation and complete mineralization of environmental pollutants.⁶ Most reports have focused on investigating the effectiveness of commercial ZnO or nanostructured ZnO powder in removing organic compounds from aqueous solution.^{7–9} However, it is worth noting that the separation of the conventional ZnO powder photocatalyst from the reacting aqueous suspension is a major problem for use in photocatalytic processes. Preparation of 1-D ZnO films, especially well-aligned ZnO nanostructure films with high stability and convenient reuse, will make it possible to overcome this disadvantage and to extend the industrial applications in environmental treatment.

For the growth of aligned 1-D ZnO nanostructures, gas-phase deposition is one of the principal technologies. Although this method can produce high-quality ZnO nanostructures, it is a high-energy-consumption route, involving thermal evaporation,¹⁰ chemical vapor deposition,¹¹ or laser ablation,¹² for example. Alternatively, solution-phase approaches to ZnO films are appealing because they are simple, low-temperature, versatile

synthetic processes and have great potential for scaleup. Li et al. successfully fabricated highly oriented hexagonal ZnO nanorod arrays on Si wafers through a two-step process, comprising the coating of the substrate with nanosized ZnO seeds by atomic layer deposition (ALD) followed by the growth of ZnO nanorod arrays on the seed-coated substrate in an aqueous solution of zinc ions.¹³ Although this is an effective method for preparing well-oriented ZnO nanorod arrays, the process is more complicated than the other approaches. In contrast, Wu et al. reported a one-step method for growing highly oriented uniform 1-D ZnO nanorod arrays by oxidation of a zinc foil in an alkaline aqueous zincate ion $[\text{Zn}(\text{OH})_4^{2-}]$ solution.¹⁴ Wang et al. directly synthesized ZnO nanorod arrays on a zinc substrate from an alcohol solution containing NaOH and cetyl trimethylammonium bromide (CTAB).¹⁵ These are regarded as important works for their simple and convenient one-step approach and for using the substrate as a reactant source.

Herein, we present an easy approach for the growth of well-aligned and high-quality 1-D ZnO nanorod arrays over a large area by the direct oxidation of zinc foil in an aqueous solution of formamide. This is a simple, self-sourced, and low-cost method without the need for precasting ZnO nanoparticles onto the substrates as a seed layer and adding materials such as Zn^{2+} -containing salts. The structural and optical properties of the as-synthesized samples were characterized and studied. Furthermore, their photocatalytic activities and stabilities were investigated in detail by the degradation of 4-chlorophenol (4-CP) in aqueous solutions.

2. Experimental Section

2.1. Fabrication of ZnO Nanorod Arrays and ZnO Nanorod Film. For the preparation of highly oriented ZnO nanorod arrays, a typical easy process was as follows: A piece of zinc foil substrate ($20 \times 40 \times 0.25$ mm³, cleaned by

* Corresponding author. Tel.: +86-411-8470-7733. Fax: +86-411-8470-8084. E-mail: xinyongli@hotmail.com.

[†] Dalian University of Technology.

[‡] Hong Kong University of Science & Technology.

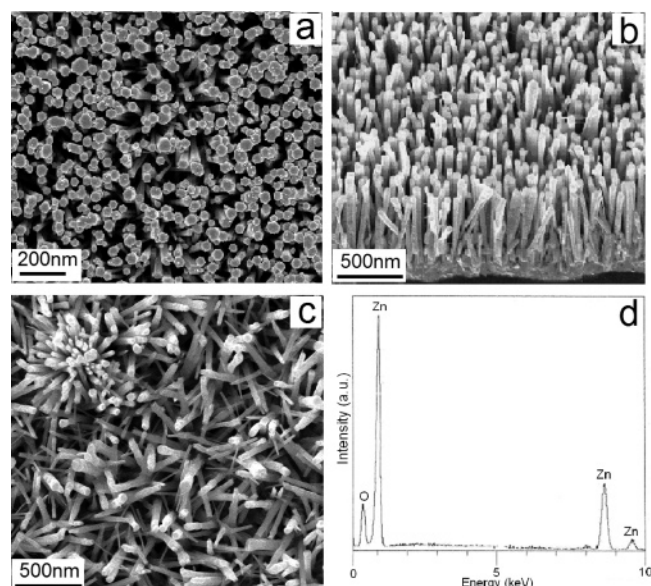


Figure 1. SEM images of (a) ZnO nanorod arrays on zinc foil and (c) ZnO nanorod film on Ti substrate. (b) Typical cross-sectional image of the arrays. (d) Corresponding EDS pattern of the arrays.

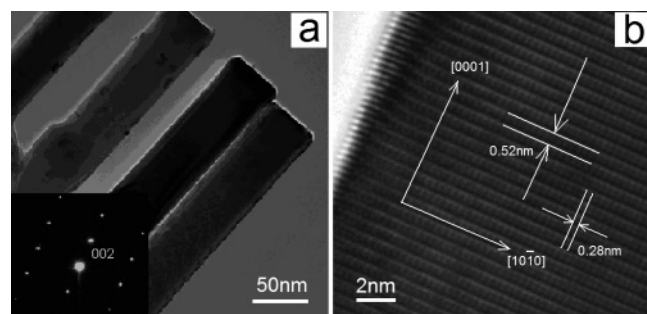


Figure 2. (a) TEM and (b) HRTEM images of ZnO nanorod arrays. The inset in part a is the SAED pattern of a single nanorod.

sonication in absolute ethanol and deionized water) was suspended and immersed in 100 mL of 5% formamide aqueous solution (v/v). In the fabrication of the ZnO nanorod film, the zinc foil was replaced by a Ti substrate, and $\text{Zn}(\text{NO}_3)_2 \cdot 6\text{H}_2\text{O}$ (0.5 M) was also added to the aqueous solution. The reaction system was then maintained at a constant temperature of 65 °C for 24 h. Then, the Zn foil (or Ti) substrate was removed, rinsed with absolute ethanol, and finally dried in air for further characterization.

2.2. Characterization. The morphology and composition of the samples were examined by scanning electron microscopy (SEM, JSM-5600 LV) combined with energy dispersive spectroscopy (EDS). Transmission electron microscopy (TEM) images, high-resolution TEM (HRTEM) images, and selected-area electron diffraction (SAED) patterns were obtained with a Tecnai G²20 transmission electron microscope at an accelerating voltage of 200 kV. X-ray diffraction (XRD) patterns were obtained on a Rigaku D/max diffractometer with Cu K α radiation ($\lambda = 0.15418$ nm). Light absorption properties were measured using a UV-vis diffuse reflectance spectrometer (JASCO, UV-550) in the wavelength range of 200–800 nm. Raman spectroscopy was conducted with a micro-Raman/photoluminescence system (Reinishaw model 3000). An argon ion laser beam with a wavelength of 514.5 nm and a power of 0.5 mW was focused on a 2- μm spot on the ZnO sample plate near the strain gauge, while the strain on the upper plane was determined by a digital strain meter (TML, TC-21k). The Raman spectroscope was calibrated and checked using a silicon sample

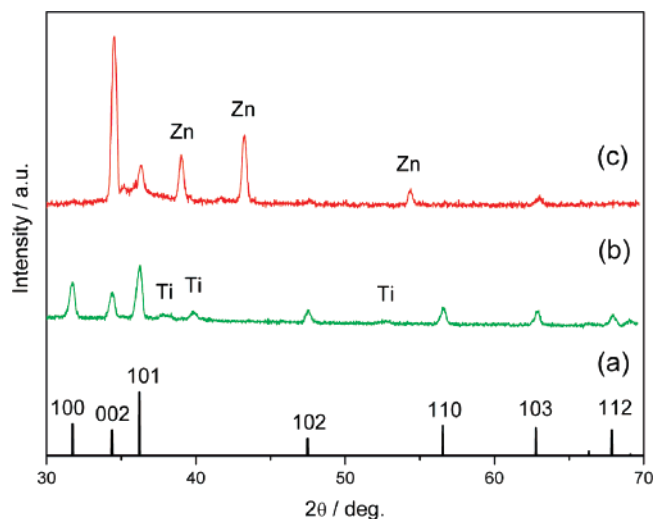


Figure 3. XRD patterns of (a) standard bulk wurtzite ZnO, (b) ZnO nanorod film on Ti substrate, and (c) ZnO nanorod arrays on zinc foil.

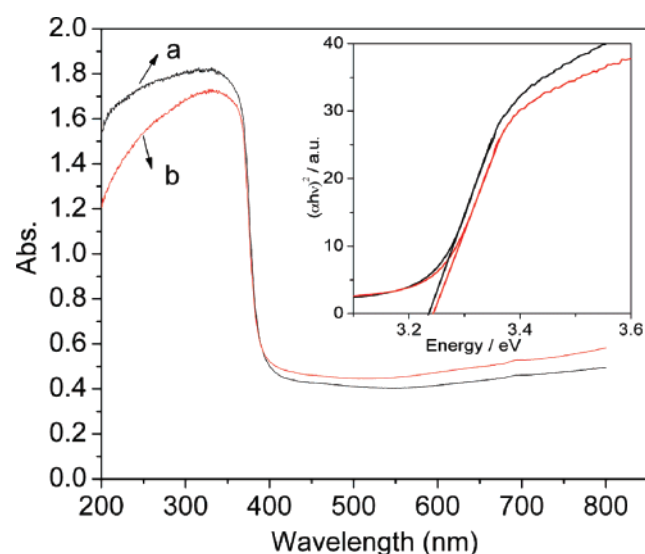


Figure 4. UV-vis diffuse reflectance spectra and plots of $(\alpha h\nu)^2$ vs the energy of absorbed light (inset) of (a) ZnO nanorod arrays on zinc foil and (b) ZnO nanorod film on Ti substrate.

before and after the ZnO spectra were recorded. Photoluminescence spectra were measured at room temperature on a Hitachi FL-4500 fluorescence spectrometer using a Xe lamp with an excitation wavelength of 350 nm.

2.3. Measurements of Photocatalytic Activities. The photocatalytic activities of the as-prepared ZnO nanorod arrays and ZnO nanorod film were evaluated by degradation of 4-CP under UV light irradiation. A 200-W high-pressure Hg lamp with a principal wavelength of 365 nm ($I_0 = 2.0$ mW·cm⁻²) was used as the UV light source. A piece of as-prepared ZnO photocatalyst was suspended upside down in a quartz reactor containing 100 mL of 4-CP ($\text{C}_6\text{H}_4\text{ClO}$, 50 mg/L) solution. Before illumination, the suspensions were magnetically stirred in the dark for 30 min to ensure adsorption equilibrium of 4-CP with the catalyst, after which they were exposed to UV light. After successive applications of stirring and irradiation, 1-mL reaction samples were withdrawn periodically for UV analysis.

3. Results and Discussion

The morphology of a ZnO nanorod arrays grown on a zinc foil substrate is shown in Figure 1a,b. Overall, highly oriented

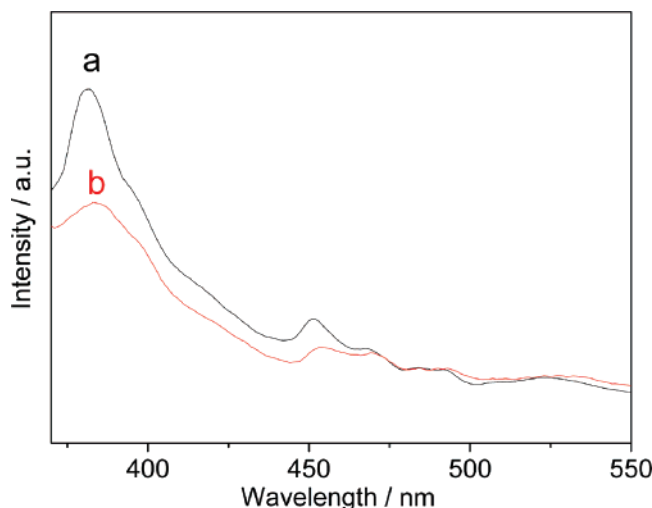


Figure 5. Room-temperature photoluminescence spectra of (a) ZnO nanorod arrays on zinc foil and (b) ZnO nanorod film on Ti substrate.

and dense ZnO hexagonal nanorods with diameters of 50 nm are aligned on the Zn foil surface, forming large-scale uniform arrays (Figure 1a). The tips of the nanorods show a flat hexagonal section, which is different from the results of Chang et al.,¹⁵ who reported sharp tips for the nanorod arrays. Cross-sectional SEM observation of the ZnO nanorod arrays (Figure 1b) reveals that rods with typical lengths of about 500 nm are separated from each other but densely aligned and that highly preferential growth occurs along the *c*-axis orientation (perpendicular to the zinc foil substrate). However, in the case of the Ti substrate, dense hexagonal ZnO nanorods can also be observed (Figure 1c), but they are packed in a disordered manner. Moreover, the ZnO nanorods also assembled into some flowerlike microstructures. These results indicate that the zinc foil is used not only as a substrate but also as a zinc-ion source for the direct growth of the ZnO nanorod arrays and plays an important role in the formation of highly oriented ZnO nanorod arrays. Figure 1d shows typical EDS results for the composition of the ZnO nanorod arrays grown on the zinc foil substrate. It reveals the presence of Zn and O as the only elementary components, with a slight oxygen deficiency (Zn/O atomic ratio \approx 1:1).

Further structural characterization of the ZnO nanorod arrays grown on the zinc foil substrate was performed by TEM. Figure 2a displays a typical TEM image of several ZnO nanorods, which is in good agreement with the SEM results, as they exhibit a uniform diameter along their entire length. The inset of Figure 2a shows the corresponding SAED pattern of a single nanorod, which indicates that the ZnO nanorod is single-crystalline in structure, according to the features of the diffraction pattern. Furthermore, the HRTEM image (Figure 2b) of the tip of an individual ZnO nanorod reveals that clear lattice spacings of 0.52 and 0.28 nm correspond to the interplanar spacings of the wurtzite ZnO (0001) and $\{10\bar{1}0\}$ planes, respectively, which also indicates that the ZnO nanorod growth occurs preferentially along the [0001] direction.

Figure 3 shows an XRD pattern of the as-synthesized samples. Figure 3a is the standard powder diffraction pattern (JCPDS 36-1451). For the ZnO nanorod film on the Ti substrate (Figure 3b), all of the diffraction peaks in the pattern can be exactly indexed as the hexagonal wurtzite ZnO with lattice constants $a = 0.3249$ nm and $c = 0.5206$ nm, which are in good agreement with the standard pattern. On the other hand, for the ZnO nanorod arrays on zinc foil (Figure 3c), all of the diffraction

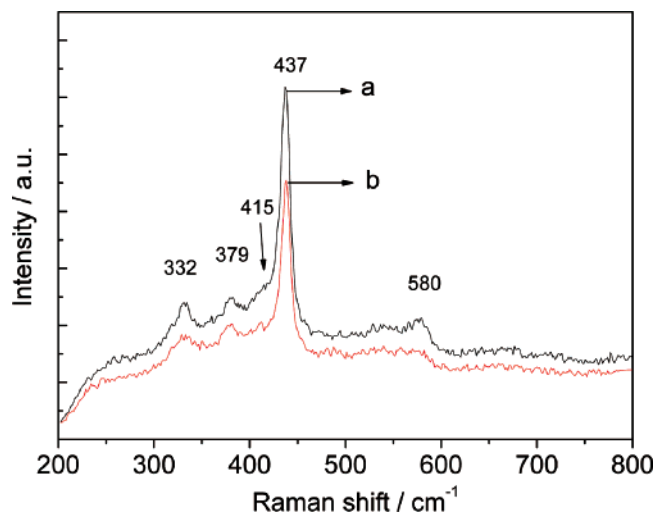


Figure 6. Raman spectra of (a) ZnO nanorod arrays on zinc foil and (b) ZnO nanorod film on Ti substrate.

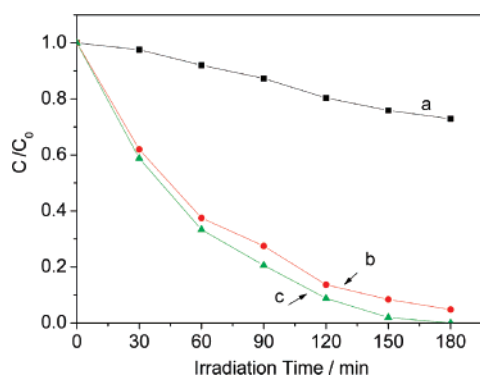


Figure 7. Progress of photocatalytic degradation of 4-CP under UV light illumination ($I_0 = 2 \text{ mW} \cdot \text{cm}^{-2}$) by (a) direct photolysis without any photocatalyst, (b) ZnO nanorod film on Ti substrate, and (c) ZnO nanorod arrays on zinc foil.

peaks can also be indexed to wurtzite-structured ZnO, except for those identified as Zn coming from the zinc substrate. Notably, when compared with the standard diffraction pattern, the (002) diffraction peaks are enhanced and much stronger than the other peaks, indicating the highly preferential growth of the ZnO nanorods along their *c* axis, perpendicular to the substrate surface.

UV-vis diffuse reflectance spectra of ZnO nanorod arrays and ZnO nanorod film are presented in Figure 4. They show similar broad and strong absorptions with a maximum at about 390 nm, which is characteristic of ZnO wide-band semiconductor material. The inset shows a plot of $(\alpha h\nu)^2$ against the energy of absorbed light, from which the direct allowed band gaps can be estimated. Using this method, the estimated band gaps of the ZnO nanorod arrays and ZnO nanorod film were found to be 3.24 and 3.23 eV, respectively. Compared with bulk ZnO (3.37 eV), the absorption edges of ZnO nanorod arrays and ZnO nanorod film are red-shifted.

Photoluminescence (PL) spectroscopy is an effective technique for evaluating the optical properties of semiconductor materials. Figure 5a shows a typical room-temperature PL spectrum of the ZnO nanorod arrays, with a dominant emission peak centered at 383 nm, which corresponds to the ultraviolet (UV) emission of ZnO with a band gap of 3.24 eV. Generally, the UV emission peak of ZnO is attributed to the near-band-edge (NBE) emission of wide-band-gap ZnO.¹⁷ In addition to

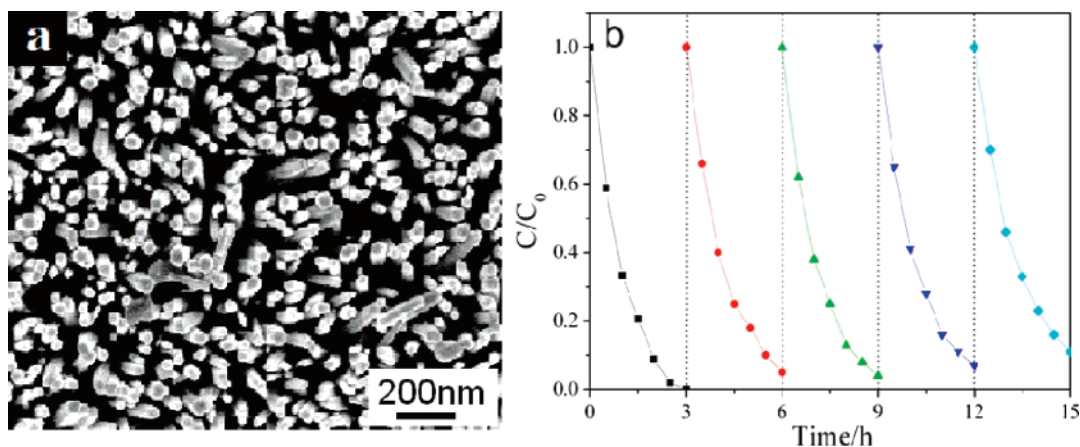


Figure 8. (a) SEM image of ZnO nanorod arrays on zinc foil after five repeated experiments. (b) Cyclic photodegradation of 4-chlorophenol under UV light irradiation. {[4-CP]₀ = 50 mg·L⁻¹, irradiation with 365-nm UV light ($I_0 = 2.0 \text{ mW} \cdot \text{cm}^{-2}$)}.

the UV emission, two weak emissions at 450 and 468 nm also can be observed for the as-grown sample. The weak peaks in the blue-green band result from an electronic transition from the level of the ionized oxygen vacancies to the valence band.¹⁸ For the ZnO nanorod film, however, a relatively weak and broad UV emission and similar blue-green emission were observed (Figure 5b), suggesting that the optical properties of ZnO crystals are sensitive to the crystal morphology.

To provide additional information on the optical properties of the as-synthesized samples, the UV Raman scattering measurements were used to investigate the vibrational properties of the ZnO nanorod arrays and ZnO nanorod film at room temperature (Figure 6). It can be seen that all of their spectroscopic peaks are almost uniform. The remarkable E_{2H} mode of ZnO is located at 437 cm^{-1} , which corresponds to the characteristic band of the hexagonal wurtzite phase. Weaker peaks appear at 332 , 379 , and 415 cm^{-1} and can be assigned to the $3E_{2H} - E_{2L}$, $A_1(\text{TO})$, and $E_1(\text{TO})$ modes of ZnO, respectively.¹⁹ In addition, the appearance of the $E_1(\text{LO})$ mode at 580 cm^{-1} , which is associated with oxygen deficiency, indicates that both the ZnO nanorod arrays and the ZnO nanorod film have a certain level of oxygen vacancies.²⁰

The photocatalytic activities of the ZnO nanorod arrays and ZnO nanorod film were measured in the photocatalytic degradation of 4-CP solution under UV light irradiation. As can be clearly seen in Figure 7, after 3 h of irradiation, the 4-CP in aqueous solution can be almost completely eliminated by the ZnO nanorod arrays, whereas the degradation effectiveness of the ZnO nanorod film and the direct photolytic process without any photocatalyst are 95% and 27%, respectively. This result illustrates that both types of photocatalysts have high photocatalytic activities. However, the ZnO nanorod arrays have a higher efficiency than the ZnO nanorod film of up to 5% in 3 h. The enhanced photocatalytic activity can be ascribed to the unique surface features of its well-aligned structure perpendicular to the zinc foil substrate. It is precisely the excess appearance of the polar ZnO (0001) faces in the ZnO nanorod arrays, which are the most active sites for photocatalytic degradation of organic pollutants, that leads to the significant enhancement of the photocatalytic activity.²¹ This result could prompt the potential application of our ZnO nanorod arrays to the treatment of wastewater.

Compared with reported ZnO photocatalysts,^{7–9} the as-prepared ZnO nanorod arrays obtained by self-sourced growth on zinc foil substrate have better stability. This allows the convenient recycling of the catalysts with cleaning by ultra-

sonication (KQ3200DB, 150W) for 3 min after each run, after which an SEM image of the ZnO nanorod arrays was taken. As shown in Figure 8a, the ZnO nanorod arrays can still be observed, and the ZnO nanorod array photocatalysts exhibit remarkable photocatalytic stability with little loss in their photocatalytic activity even after five cycles (Figure 8b).

4. Conclusion

In summary, well-aligned ZnO nanorod arrays have been fabricated on a large scale by a one-step wet chemical approach using the natural direct oxidation of zinc foil in formamide/water solution. The structure of the ZnO nanorod arrays was single-crystalline and grown along the *c*-axis orientation. PL and Raman spectra show that these ZnO nanorod arrays have good optical properties. The ZnO nanorod arrays exhibit enhanced photocatalytic properties compared to those of ZnO nanorod films, as demonstrated in the photodegradation of 4-CP in aqueous solution. These ZnO nanorod arrays with good optical properties and photocatalytic activities and improved stability should find potential applications in photocatalysis, solar cell, and purification processes.

Acknowledgment. This work was jointly supported by the National Nature Science Foundation of China (20677007), National High-tech Project 863 (2007AA061402), and National Key Basic Research Project 973 (2007CB613302).

References and Notes

- (1) Huang, M. H.; Mao, S.; Feick, H.; Yan, H.; Wu, Y.; Kind, H.; Weber, E.; Russo, R.; Yang, P. *Science* **2001**, *292*, 1897.
- (2) Rodriguez, J. A.; Jirsak, T.; Dvorak, J.; Sambasivan, S.; Fischer, D. *J. Phys. Chem. B* **2000**, *104*, 319.
- (3) Liu, C. H.; Zapien, J. A.; Yao, Y.; Meng, X. M.; Lee, C. S.; Fan, S. S.; Lifshitz, Y.; Lee, S. T. *Adv. Mater.* **2003**, *15*, 838.
- (4) Law, M.; Greene, L. E.; Johnson, J. C.; Saykally, R.; Yang, P. D. *Nat. Mater.* **2005**, *4*, 455.
- (5) Hariharan, C. *Appl. Catal. A: Gen.* **2006**, *304*, 55.
- (6) Yeber, M. C.; Rodriguez, J.; Freer, J.; Duran, N.; Mansilla, H. D. *Chemosphere* **2000**, *41*, 1193.
- (7) Chen, C. C. *J. Mol. Catal. A: Chem.* **2007**, *264*, 82.
- (8) Parida, K. M.; Dash, S. S.; Das, D. P. *J. Colloid Interface Sci.* **2006**, *298*, 787.
- (9) Nishio, J.; Tokumura, M.; Znad, H. T.; Kawase, Y. *J. Hazard. Mater.* **2006**, *138*, 106.
- (10) Gao, P. X.; Wang, Z. L. *Small* **2005**, *1*, 945.
- (11) Zhang, Z. X.; Yuan, H. J.; Zhou, J. J.; Liu, D. F.; Luo, S. D.; Miao, Y. M.; Gao, Y.; Wang, J. X.; Liu, L. F.; Song, L. *J. Phys. Chem. B* **2006**, *110*, 8566.
- (12) Kawakami, M.; Hartanto, A. B.; Nakata, Y.; Okada, T. *Jpn. J. Appl. Phys.* **2003**, *42*, L33.

- (13) Li, Q. C.; Kumar, V.; Li, Y.; Zhang, H. T.; Marks, T. J.; Chang, R. P. H. *Chem. Mater.* **2005**, *17*, 1001.
- (14) Wu, X. F.; Bai, H.; Li, C.; Lu, G. W.; Shi, G. Q. *Chem. Commun.* **2006**, *15*, 1655.
- (15) Wang, D. G.; Song, C. X. *J. Phys. Chem. B* **2005**, *109*, 12697.
- (16) Chang, Y. C.; Chen, L. J. *J. Phys. Chem. C* **2007**, *111*, 1268.
- (17) Wu, J. J.; Liu, S. C. *Adv. Mater.* **2002**, *14*, 215.
- (18) Zhang, D. H.; Wang, Q. P.; Xue, Z. Y. *Appl. Surf. Sci.* **2003**, *207*, 20.
- (19) Damen, T. C.; Porto, S. P. S.; Tell, B. *Phys. Rev.* **1966**, *142*, 570.
- (20) Chen, S. J.; Liu, Y. C.; Shao, C. L.; Mu, R.; Lu, Y. M.; Zhang, J. Y.; Shen, D. Z.; Fan, X. W. *Adv. Mater.* **2005**, *17*, 586.
- (21) Jang, E. S.; Won, J. H.; Hwang, S. J.; Choy, J. H. *Adv. Mater.* **2006**, *18*, 3309.